Inorg. Chem. **2005**, *44*, 6211–6218

Electronic Spectra of Pure Uranyl(V) Complexes: Characteristic Absorption Bands Due to a $U^VO_2^+$ Core in Visible and Near-Infrared Regions[1]

Koichiro Mizuoka,[†] Satoru Tsushima,[‡] Miki Hasegawa,[§] Toshihiko Hoshi,[§] and Yasuhisa Ikeda*,[†]

Research Laboratory for Nuclear Reactors, Tokyo Institute of Technology, 2-12-1-N1-34 O-okayama, Meguro-ku, Tokyo 152-8550, Japan, The Albanova University Center, Institute of Physics, Stockholm University, S-106 91 Stockholm, Sweden, and Department of Chemistry and Biological Science, College of Science and Engineering, Aoyama-Gakuin University, Fuchinobe, Sagamihara, Kanagawa 229-8558, Japan

Received March 14, 2005

To clarify the electronic spectral properties of uranyl(V) complexes systematically, we measured absorption spectra of three types of pure uranyl(V) complexes: $[U^VO_2(dbm)_2DMSO]^-$, $[U^VO_2(saloph)DMSO]^-$, and $[U^VO_2(CO_3)_3]^{5-}$ (dbm = dibenzoylmethanate, saloph = *N,N′*-disalicylidene-*o*-phenylenediaminate, DMSO = dimethyl sulfoxide). As a result, it was found that these uranyl(V) complexes have characteristic absorption bands in the visible–near-infrared (NIR) region, i.e., at around 640, 740, 860, 1470, and 1890 nm (molar absorptivity, ϵ = 150–900 $M^{-1}\cdot cm^{-1}$) for $[U^VO_2(dbm)_2DMSO]^-$, 650, 750, 900, 1400, and 1875 nm (ϵ = 100–300 $M^{-1}\cdot cm^{-1}$) for $[U^VO_2(saloph)DMSO]^-$, and 760, 990, 1140, 1600, and 1800 nm (ϵ = 0.2–3.6 $M^{-1}\cdot cm^{-1}$) for $[U^VO_2(CO_3)_3]^{5-}$. These characteristic absorption bands of the uranyl(V) complexes are attributable to the electronic transitions in the $U^VO_2^+$ core because the spectral features are similar to each other despite the differences in the ligands coordinated to the equatorial plane of the $U^VO_2^+$ moiety. On the other hand, the ϵ values of $[U^VO_2(CO_3)_3]^{5-}$ are quite smaller than those of $[U^VO_2(dbm)_2DMSO]^-$ and $[U^VO_2(saloph)DMSO]^-$. Such differences can be explained by the different coordination geometries around the center uranium in these uranyl(V) complexes. Consequently, the absorption bands of the uranyl(V) complexes in visible–NIR region were assigned to f–f transitions in the $5f^1$ configuration.

1. Introduction

Actinide elements at higher oxidation states than 5+ exist as actinyl ions (AnO_2^{n+}, An = U, Np, Pu, Am). In AnO_2^{n+}, the uranyl(V) ion ($U^VO_2^+$) has one unpaired electron in the 5f orbital ($5f^1$), which is the simplest electronic configuration in AnO_2^{n+} species. Therefore, the knowledge concerning the fundamental properties of the U(V) species should be useful for the systematic interpretation of characteristics of AnO_2^{n+}. Nevertheless, only limited data for the U(V) species are available because the U(V) species are generally unstable in solutions for disproportionation to U(IV) and U(VI) species.[2] Electronic spectral studies on the U(V) species in aqueous and nonaqueous systems have been attempted by photochemical and electrochemical reduction of U(VI) complexes to U(V) ones.[3−10] As a result, it has been proposed that the U(V) species have characteristic absorption bands at around 650, 750, 1000, and 1500 nm (15 400, 13 300,

* To whom correspondence should be addressed. E-mail: yikeda@nr.titech.ac.jp. Phone and Fax: +81-3-5734-3061.
[†] Tokyo Institute of Technology.
[‡] Stockholm University.
[§] Aoyama-Gakuin University.

(1) Mizuoka, K.; Tsushima, S.; Hasegawa, M.; Hoshi, T.; Ikeda, Y. XXXVIth International Conference on Coordination Chemistry (ICCC36), Merida, Mexico, O5.46, 2004.
(2) (a) Heal, H. G. *Trans. Faraday Soc.* **1949**, *45*, 1−11. (b) Heal, H. G.; Thomas, J. G. N. *Trans. Faraday Soc.* **1949**, *45*, 11−20. (c) Newton, T. W.; Baker, F. B. *Inorg. Chem.* **1974**, *13*, 1166−1170. (d) Ekstrom, A. *Inorg. Chem.* **1974**, *13*, 2237−2241. (e) McDuffie, B.; Reilley, C. N. *Anal. Chem.* **1966**, *38*, 1881−1887.
(3) Gritzner, G.; Selbin, J. *J. Inorg. Nucl. Chem.* **1968**, *30*, 1799.
(4) Selbin, J.; Ortego, J. D. *Chem. Rev.* **1969**, *69*, 657.
(5) Bell, J. T.; Friedman, H. A.; Billings, M. R. *J. Inorg. Nucl. Chem.* **1974**, *36*, 2563.
(6) Kaneki, H.; Fukutomi, H. *Bull. Res. Lab. Nucl. React. (Tokyo Inst. Technol.)* **1980**, *5*, 27.
(7) Folcher, G.; Lambard, J.; Villardi, G. C. *Inorg. Chim. Acta* **1980**, *45*, L59.
(8) Miyake, C.; Yamana, Y.; Imoto, S. *Inorg. Chim. Acta* **1984**, *95*, 17.
(9) Miyake, C.; Kondo, T.; Imoto, S. *J. Less-Common Met.* **1986**, *122*, 313.
(10) Monjushiro, H.; Hara, H.; Yokoyama, Y. *Polyhedron* **1992**, *11*, 845.

10.1021/ic0503838 CCC: $30.25
Published on Web 08/11/2005

10 000, and 6700 cm^{-1}). However, the sample solutions in most of the previous reports were mixtures of U(IV), U(V), and U(VI).

On the other hand, it has been reported that some U(V) species might be produced stably in molten alkali and alkaline-earth chloride mixtures.[11,12] Adams et al. reported that the U(V) species in LiCl−KCl, LiCl−$MgCl_2$, and NaCl−KCl−$MgCl_2$ eutectics show similar electronic spectra at around 690, 870, and 1510 nm (14 500, 11 500, and 6620 cm^{-1}).[11] Furthermore, Khokhryakov also observed that the U(V) species in CsCl−NaCl and NaCl−KCl melts have absorption bands at around 615, 715, and 1560 nm (16 300, 14 000, and 6410 cm^{-1}) and tried to assign them.[12] However, the coordination structures around the $U^VO_2^+$ ion in the molten salt systems have not been identified.

In such a situation, Cohen found the stable U(V) species in a basic carbonate aqueous solution (pH > 11)[13] and reported that the sample solution containing the U(V) carbonate is colorless. By using a spectroelectrochemical technique with an optical transparent thin layer electrode (OTTLE) cell,[14] we have also confirmed the disappearance of the absorption bands due to a charge transfer from the axial oxygen to the center uranium (ligand-to-metal charge transfer, LMCT) in $[U^{VI}O_2(CO_3)_3]^{4-}$ at around 450 nm (22 000 cm^{-1}) with the reduction from U(VI) to U(V) in aqueous solution containing Na_2CO_3 [1 mol·dm^{-3} (M)].[15] The potentiometric,[16] EXAFS,[17] and ^{13}C NMR[18] studies have determined the stoichiometry and structure of the uranyl(V) carbonate as $[U^VO_2(CO_3)_3]^{5-}$, which is similar to the hexagonal-bipyramidal structure of $[U^{VI}O_2(CO_3)_3]^{4-}$ (Chart 1). For the spectroscopic properties of $[U^VO_2(CO_3)_3]^{5-}$ in the visible−near-infrared (NIR) region, Cohen reported that $[U^VO_2(CO_3)_3]^{5-}$ has characteristic absorption bands at around 765, 990, and 1120 nm (13 100, 10 100, and 8930 cm^{-1}).[13] However, the absorption spectrum in the energy region lower than 1350 nm (7410 cm^{-1}) has not been observed because of the strong absorption of H_2O as the solvent. Because no other stable U(V) species with identified structures, except for $[U^VO_2(CO_3)_3]^{5-}$, are known, the spectroscopic properties of the U(V) complexes have not been discussed systematically.

Recently, we investigated the electrochemical and spectroelectrochemical properties of $U^{VI}O_2$(saloph)DMSO (saloph = *N*,*N*′-disalicylidene-*o*-phenylenediaminate, DMSO = dimethyl sulfoxide) in DMSO.[19,20] As a result, it was clarified

Chart 1. Structures of U(V/VI) Complexes and Ligands

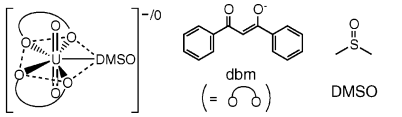

$[U^VO_2(dbm)_2DMSO]^-/U^{VI}O_2(dbm)_2DMSO$

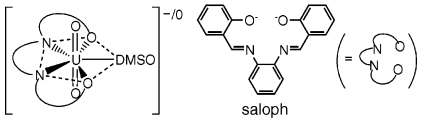

$[U^VO_2(saloph)DMSO]^-/U^{VI}O_2(saloph)DMSO$

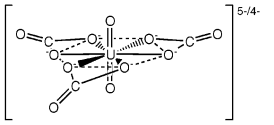

$[U^VO_2(CO_3)_3]^{5-}/[U^{VI}O_2(CO_3)_3]^{4-}$

that the U(V) complex, $[U^VO_2(saloph)DMSO]^-$, is produced as a stable and pure species by the electrochemical reduction of $U^{VI}O_2$(saloph)DMSO in a DMSO solution and that the U═O bond strength in the uranyl moiety is weakened with the reduction. This is the first example of a stable U(V) complex in a nonaqueous solvent. The formal potential ($E^{\circ\prime}$) of the redox couple $[U^VO_2(saloph)DMSO]^-/U^{VI}O_2$(saloph)-DMSO was evaluated as −1.550 V vs Fc/Fc^+ (ferrocene/ferrocenium ion redox couple).

More recently, we studied the electrochemical and IR spectroelectrochemical properties of $U^{VI}O_2(dbm)_2$DMSO (dbm = dibenzoylmethanate) in DMSO.[21] The resulting cyclic voltammograms indicated that $U^{VI}O_2(dbm)_2$DMSO is reduced to $[U^VO_2(dbm)_2DMSO]^-$ without any successive reactions. Furthermore, IR spectra showed that an asymmetric stretching band of the uranyl moiety shifts to lower wavenumber with the reduction from $U^{VI}O_2(dbm)_2$DMSO to $[U^VO_2(dbm)_2DMSO]^-$. Thus, $[U^VO_2(dbm)_2DMSO]^-$ in DMSO was recognized as the second example of a stable U(V) complex in a nonaqueous solvent.

In the present study, to clarify the electronic spectral properties of the U(V) complexes systematically, we tried to observe the electronic spectra of three different U(V) complexes: $[U^VO_2(dbm)_2DMSO]^-$, $[U^VO_2(saloph)DMSO]^-$, and $[U^VO_2(CO_3)_3]^{5-}$ (see Chart 1).

2. Experimental Section

2.1. Materials. The U(VI) complexes ($U^{VI}O_2$(saloph)DMSO, $U^{VI}O_2(dbm)_2$DMSO, and $Na_4[U^{VI}O_2(CO_3)_3]$) as starting materials were prepared according to previous papers.[19,21,22] DMSO (Kanto Chemical Co., Ind.) was distilled under vacuum after drying with CaH_2 (Wako Pure Chemical Ind., Ltd.) and stored over molecular sieves 4A (Wako). As supporting electrolytes, tetra-*n*-butylammonium perchlorate (TBAP; Fluka, electrochemical grade) and Na_2CO_3 (Kanto) were used without further purification. Deuterium oxide (D_2O; 99.8 atom % D, Acros) was utilized as a solvent for the $[U^VO_2(CO_3)_3]^{5-}/[U^{VI}O_2(CO_3)_3]^{4-}$ system. All other chemicals were of reagent grade.

(11) Adams, M. D.; Wenz, D. A.; Steunenberg, R. K. *J. Phys. Chem.* **1963**, *67*, 1939.
(12) Khokhryakov, A. A. *Radiochemistry (Moscow, Russ. Fed.)* **1998**, *40*, 413.
(13) Cohen, D. *J. Inorg. Nucl. Chem.* **1970**, *32*, 3525.
(14) Heineman, W. R. *J. Chem. Educ.* **1983**, *60*, 305.
(15) Mizuguchi, K.; Park, Y.-Y.; Tomiyasu, H.; Ikeda, Y. *J. Nucl. Sci. Technol.* **1993**, *30*, 542.
(16) Ferri, D.; Grenthe, I.; Salvatore, F. *Inorg. Chem.* **1983**, *22*, 3162.
(17) Docrat, T. I.; Mosselmans, J. F. W.; Charnock, J. M.; Whiteley, M. W.; Collison, D.; Livens, F. R.; Jones, C.; Edmiston, M. J. *Inorg. Chem.* **1999**, *38*, 1879.
(18) Mizuoka, K.; Grenthe, I.; Ikeda, Y. *Inorg. Chem.* **2005**, *44*, 4472.
(19) Mizuoka, K.; Kim, S.-Y.; Hasegawa, M.; Hoshi, T.; Uchiyama, G.; Ikeda, Y. *Inorg. Chem.* **2003**, *42*, 1031.
(20) Mizuoka, K.; Ikeda, Y. *Inorg. Chem.* **2003**, *42*, 3396.
(21) Mizuoka, K.; Ikeda, Y. *Radiochim. Acta* **2004**, *92*, 631.
(22) Brittain, H. G.; Tsao, L.; Perry, D. L. *J. Lumin.* **1984**, *29*, 285.

A stock solution containing $[U^{V}O_2(CO_3)_3]^{5-}$ (5.5×10^{-2} M) was prepared by the electrochemical reduction of $[U^{VI}O_2(CO_3)_3]^{4-}$ in a D_2O solution containing Na_2CO_3 (1 M). The sample solution was deoxygenated by passing dry argon gas for 3 h prior to the bulk electrolysis, and the argon gas was passed through the sample solution during the electrolysis. The applied potential on a Pt plate working electrode was −0.950 V vs Ag/AgCl.[23] All operations for the preparation and sampling of $[U^{V}O_2(CO_3)_3]^{5-}$ were performed in a glovebox under an argon atmosphere at 298 K. In our recent study,[18] it was already confirmed that, in the ^{13}C NMR spectrum of the resulting sample solution prepared by this bulk electrolysis, the signals of $[U^{V}O_2(CO_3)_3]^{5-}$ (106.70 ppm) and free CO_3^{2-} (169.13 ppm) are observed without that of $[U^{VI}O_2(CO_3)_3]^{4-}$ (168.22 ppm); i.e., $[U^{V}O_2(CO_3)_3]^{5-}$ is purely produced.

2.2. Method. Spectroelectrochemical measurements for $[U^{V}O_2(dbm)_2DMSO]^{-}/U^{VI}O_2(dbm)_2DMSO$ and $[U^{V}O_2(saloph)$-$DMSO]^{-}/U^{VI}O_2(saloph)DMSO$ were carried out with spectrophotometers (UV−visible region, Agilent 8453; visible−NIR region, Shimadzu UV-3150) equipped with OTTLE cells.[24] The optical path lengths of the OTTLE cells for Agilent 8453 and Shimadzu UV-3150 were spectrophotometrically calibrated as 2.80×10^{-2} and 1.89×10^{-2} cm, respectively. The three-electrode system was utilized in each OTTLE cell, that is, a Pt minigrid working electrode as the OTTLE, a Pt counter electrode (BAS 002222), and an Ag/AgCl reference electrode (BAS 002020 RE-1B) with a liquid junction. The applied potential on the OTTLE was controlled by a BAS CV-50W voltammetric analyzer. The electronic spectra at various applied potentials were measured after equilibrium of the electrochemical reaction on the OTTLE at 298 K was reached, which required 2 min. The sample solutions in the OTTLE cells were deoxygenated by passing dry argon gas at least 1 h prior to the measurements.

The electronic spectra of D_2O solutions containing $[U^{V}O_2(CO_3)_3]^{5-}$ and $[U^{VI}O_2(CO_3)_3]^{4-}$ in a tightly sealed 1-cm quartz cell were measured by using a Shimadzu UV-3150 spectrophotometer.

3. Results and Discussion

3.1. UV−Visible−NIR Spectroelectrochemistry for $[U^{V}O_2(dbm)_2DMSO]^{-}/U^{VI}O_2(dbm)_2DMSO$ in DMSO. In the previous study, we reported that $U^{VI}O_2(dbm)_2DMSO$ in DMSO is quasi-reversibly reduced to $[U^{V}O_2(dbm)_2DMSO]^{-}$ at around −1.362 V vs Fc/Fc^{+} and that the resulting $[U^{V}O_2(dbm)_2DMSO]^{-}$ is pure and stable in DMSO.[21] To confirm this phenomenon spectrophotometrically, we performed the UV−visible spectroelectrochemical measurements of a DMSO solution containing $U^{VI}O_2(dbm)_2DMSO$ (1.04×10^{-3} M) and TBAP (0.3 M) with the OTTLE cell. The UV−visible absorption spectra were measured at the potentials varied stepwise in the range of 0 to −1.559 V vs Fc/Fc^{+}. The resulting spectra are shown in Figure 1. As can be seen from this figure, the spectral changes were observed with a decrease in the potential and converged at −1.559 V vs Fc/Fc^{+}. As a result, clear isosbestic points were detected at 260, 348, 398, and 524 nm. This result indicates that only one equilibrium exists in this system. As the most probable candidate, the redox couple of $[U^{V}O_2(dbm)_2DMSO]^{-}/U^{VI}O_2(dbm)_2DMSO$ can be proposed as reported previously.[21]

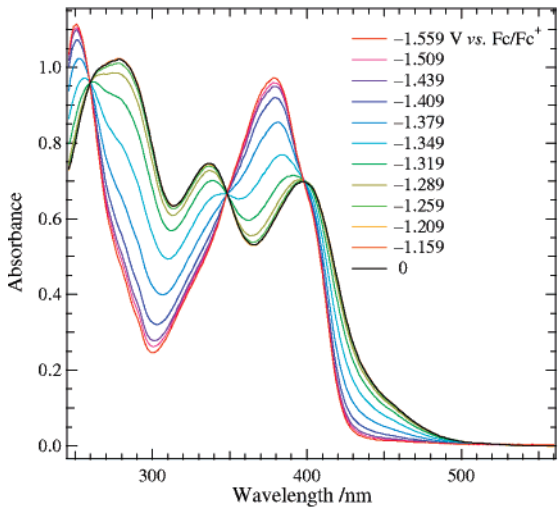

Figure 1. UV−visible absorption spectra measured at the applied potentials in the range from 0 to −1.559 V vs Fc/Fc^{+} for $U^{VI}O_2(dbm)_2DMSO$ (1.04×10^{-3} M) in a DMSO solution containing TBAP (0.3 M). Optical path length: 2.80×10^{-2} cm.

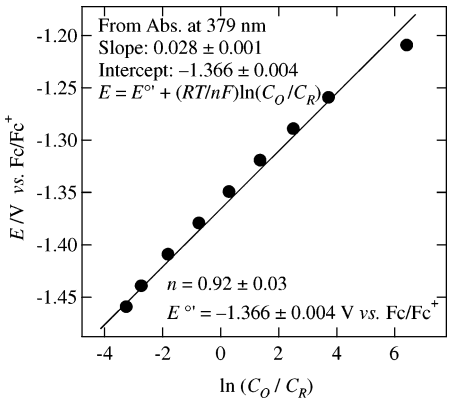

Figure 2. Nernstian plot for the absorbancies at 379 nm in Figure 1.

To determine the electron stoichiometry (n) for the redox couple in Figure 1, a Nernstian plot was performed by using the absorbancies at 379 nm in Figure 1. The result is shown in Figure 2. From the slope (0.028 ± 0.001) and intercept (−1.366 ± 0.004) of this plot, the values of n and $E^{\circ\prime}$ were evaluated as 0.92 ± 0.03 and −1.366 ± 0.004 V vs Fc/Fc^{+}, respectively. Therefore, it was confirmed that $[U^{V}O_2(dbm)_2$-$DMSO]^{-}$ is purely produced as the stable U(V) complex in DMSO. The UV−visible absorption spectrum measured at −1.559 V vs Fc/Fc^{+} in Figure 1 is assigned to pure $[U^{V}O_2(dbm)_2DMSO]^{-}$ in DMSO.

(23) Various $E^{\circ\prime}$ values of $[U^{V}O_2(CO_3)_3]^{5-}/[U^{VI}O_2(CO_3)_3]^{4-}$ were reported such as −0.714, −0.730, −0.7459, −0.749, −0.815, and −0.859 vs Ag/AgCl (summarized by Grenthe, I.; Fuger, J.; Konings, R. J. M.; Lemire, R. J.; Muller, A. B.; Nguyen-Trung, C.; Wanner, H. *Chemical Thermodynamics of Uranium*; North-Holland: Amsterdam, The Netherlands, 1992). To evaluate the $E^{\circ\prime}$ value of $[U^{V}O_2(CO_3)_3]^{5-}/[U^{VI}O_2(CO_3)_3]^{4-}$ under our experimental conditions, we performed the UV−visible spectroelectrochemical measurements for $[U^{V}O_2$-$(CO_3)_3]^{5-}/[U^{VI}O_2(CO_3)_3]^{4-}$ in a D_2O solution containing 1 M Na_2-CO_3 in a manner similar to that of $[U^{V}O_2(dbm)_2DMSO]^{-}/U^{VI}O_2(dbm)_2$-DMSO (see section 3.1). The resulting spectra and the Nernstian plot are shown in Figures S1 and S2 in the Supporting Information, respectively. The applied potential was changed in the range from 0 to −0.900 V vs Ag/AgCl. As a result, the values of the electron stoichiometry and $E^{\circ\prime}$ of $[U^{V}O_2(CO_3)_3]^{5-}/[U^{VI}O_2(CO_3)_3]^{4-}$ were evaluated as 0.90 ± 0.02 and −0.751 ± 0.001 V vs Ag/AgCl at 298 K, respectively.

(24) Endo, A.; Mochida, I.; Shimizu, K.; Satô, G. P. *Anal. Sci.* **1995**, *11*, 457.

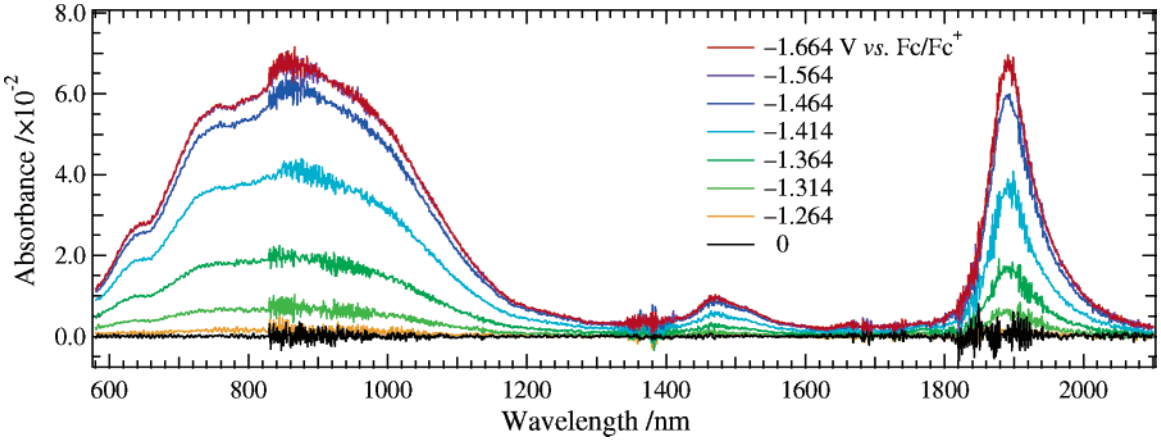

Figure 3. Visible−NIR absorption spectra measured at the applied potentials in the range from 0 to −1.664 V vs Fc/Fc^+ for $[U^VO_2(dbm)_2DMSO]^-$/$U^{VI}O_2(dbm)_2DMSO$ (4.11×10^{-3} M) in a DMSO solution containing TBAP (0.3 M). Noises are due to detectors (photomultiplier and PbS detector) in the spectrophotometer and/or absorption of DMSO in the OTTLE cell. Optical path length: 1.89×10^{-2} cm.

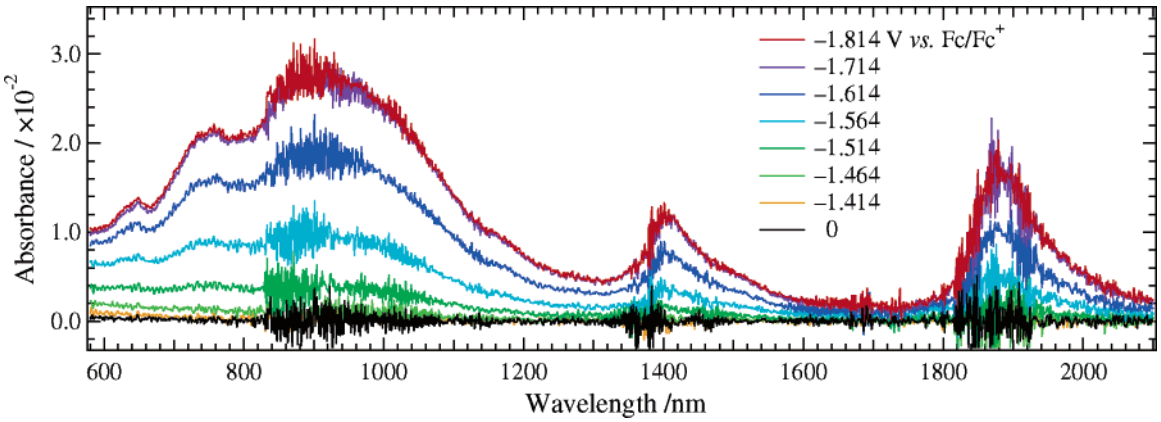

Figure 4. Visible−NIR absorption spectra measured at the applied potentials in the range from 0 to −1.814 V vs Fc/Fc^+ for $[U^VO_2(saloph)DMSO]^-$/$U^{VI}O_2(saloph)DMSO$ (5.28×10^{-3} M) in a DMSO solution containing TBAP (0.3 M). Noises are due to detectors (photomultiplier and PbS detector) in the spectrophotometer and/or absorption of DMSO in the OTTLE cell. Optical path length: 1.89×10^{-2} cm.

To obtain detailed data concerning the spectroscopic property of $[U^VO_2(dbm)_2DMSO]^-$ in the visible−NIR region, we measured the visible−NIR absorption spectra for the redox couple of $[U^VO_2(dbm)_2DMSO]^-$/$U^{VI}O_2(dbm)_2DMSO$ (total concentration: 4.11×10^{-3} M) at various applied potentials in the range of 0 to −1.664 V vs Fc/Fc^+ using the spectroelectrochemical technique. The resulting spectra are shown in Figure 3. The absorption bands were observed at around 640, 740, 860, 1470, and 1890 nm with a decrease in the potential, and then the spectral changes converged at −1.564 V vs Fc/Fc^+ as well as the results in Figure 1. Therefore, it is concluded that the spectrum at −1.564 V vs Fc/Fc^+ is attributed to $[U^VO_2(dbm)_2DMSO]^-$ and that the absorption bands in Figure 3 are intrinsic ones of $[U^VO_2(dbm)_2DMSO]^-$. The molar absorptivities (ϵ) of these absorption bands are in the range from 150 to 900 $M^{-1}\cdot cm^{-1}$.

3.2. Visible−NIR Spectroelectrochemistry for $[U^VO_2(saloph)DMSO]^-$/$U^{VI}O_2(saloph)DMSO$ in DMSO. To examine whether the characteristic absorption bands of $[U^VO_2(dbm)_2DMSO]^-$ in the visible-NIR region are a common property of the U(V) complexes, we measured the visible−NIR absorption spectra for the redox couple of $[U^VO_2(saloph)DMSO]^-$/$U^{VI}O_2(saloph)DMSO$ (total concentration: 5.28×10^{-3} M) in DMSO containing TBAP (0.3 M) with the spectroelectrochemical technique. On the basis of our previous study,[19] the potential applied on the OTTLE was varied stepwise from 0 to −1.814 V vs Fc/Fc^+. The results are shown in Figure 4. Similarly to the result for the $[U^VO_2(dbm)_2DMSO]^-$/$U^{VI}O_2(dbm)_2DMSO$ couple (Figure 3), the absorbancies at around 650, 750, 900, 1400, and 1875 nm increased with the reduction of $U^{VI}O_2(saloph)DMSO$ to $[U^VO_2(saloph)DMSO]^-$, and such spectral changes converged at −1.814 V vs Fc/Fc^+. Therefore, the absorption spectrum measured at −1.814 V vs Fc/Fc^+ is assigned to $[U^VO_2(saloph)DMSO]^-$. It is clear that the absorption bands in Figure 4 are the characteristic ones of $[U^VO_2(saloph)$-$DMSO]^-$. The ϵ values of these absorption bands are in the range from 100 to 300 $M^{-1}\cdot cm^{-1}$.

In a comparison between Figures 3 and 4, the electronic spectra of $[U^VO_2(dbm)_2DMSO]^-$ and $[U^VO_2(saloph)DMSO]^-$ resemble each other despite the difference in the ligands coordinated to the equatorial plane of the $U^VO_2^+$ moiety. Such a similarity implies that the spectral changes in Figures 3 and 4 do not correspond to the reduction of the ligands (dbm, saloph, and DMSO) but the uranyl core ($U^{VI}O_2^{2+} + e^- \rightarrow U^VO_2^+$) and strongly suggests that the characteristic absorption bands of these U(V) complexes in the visible−

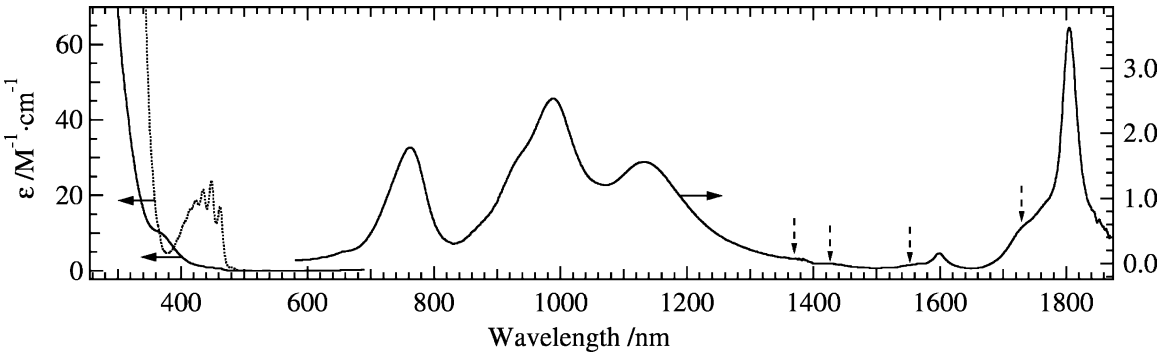

Figure 5. Electronic spectra of $[U^{V}O_2(CO_3)_3]^{5-}$ (5.5×10^{-2} M, solid line) and $[U^{VI}O_2(CO_3)_3]^{4-}$ (5.5×10^{-2} M, dotted line) in D_2O containing Na_2CO_3 (1 M). Broken arrows indicate residuals after subtraction of the spectrum due to HDO from the resulting spectrum.[25] Optical path length: 1 cm.

NIR region are primarily due to the electronic transitions in the $U^{V}O_2^{+}$ core.

3.3. Electronic Spectrum of $[U^{V}O_2(CO_3)_3]^{5-}$ in D_2O. It can be expected that $[U^{V}O_2(CO_3)_3]^{5-}$ also has the characteristic absorption bands in the visible−NIR region in analogy with $[U^{V}O_2(dbm)_2DMSO]^{-}$ and $[U^{V}O_2(saloph)DMSO]^{-}$. Actually, Cohen reported that $[U^{V}O_2(CO_3)_3]^{5-}$ has the absorption bands at around 765, 990, and 1120 nm.[13] However, it has not been confirmed whether $[U^{V}O_2(CO_3)_3]^{5-}$ as well as $[U^{V}O_2(dbm)_2DMSO]^{-}$ and $[U^{V}O_2(saloph)DMSO]^{-}$ has the absorption bands in the energy region lower than 1350 nm. Hence, we tried to measure the electronic spectrum of $[U^{V}O_2(CO_3)_3]^{5-}$ in D_2O in the range from 260 to 1870 nm by using the spectroelectrochemical technique. As a result, the electronic spectra could not be observed clearly in this technique. This is supposed to be due to the small absorptivities of $[U^{V}O_2(CO_3)_3]^{5-}$ in the visible−NIR region. Therefore, the sample solution of $[U^{V}O_2(CO_3)_3]^{5-}$ was prepared by the electrochemical reduction of $[U^{VI}O_2(CO_3)_3]^{4-}$ in D_2O containing Na_2CO_3 (1 M) (see the Experimental Section). The electronic spectrum of the resulting solution was measured in the range from 260 to 1870 nm with a conventional 1-cm quartz cell. The result is drawn with a solid line in Figure 5,[25] together with that of $[U^{VI}O_2(CO_3)_3]^{4-}$ depicted by a dotted line.

In the UV−visible region, it is found that the LMCT absorption bands of $[U^{VI}O_2(CO_3)_3]^{4-}$ at ca. 450 nm on the dotted line are not observed on the solid line. This means that $[U^{VI}O_2(CO_3)_3]^{4-}$ in the starting solution was completely reduced to $[U^{V}O_2(CO_3)_3]^{5-}$. For the sample solution of $[U^{V}O_2(CO_3)_3]^{5-}$ in the tightly sealed 1-cm quartz cell, any spectral changes from the solid line in Figure 5 were not observed over the course of several months.

In the visible−NIR region, the characteristic absorption bands of $[U^{V}O_2(CO_3)_3]^{5-}$ were observed at around 760, 990, 1140, 1600, and 1800 nm. The absorption bands at 760, 990, and 1140 nm are consistent with the results of Cohen,[13] and those at 1600 and 1800 nm in the strong absorption region of H_2O are the first observation for $[U^{V}O_2(CO_3)_3]^{5-}$. As expected above, the electronic spectral features of $[U^{V}O_2(CO_3)_3]^{5-}$ in the visible−NIR region are similar to those of $[U^{V}O_2(dbm)_2DMSO]^{-}$ and $[U^{V}O_2(saloph)DMSO]^{-}$, especially for two absorption peaks at 1600 and 1800 nm. Therefore, it is considered that the characteristic absorption bands of $[U^{V}O_2(CO_3)_3]^{5-}$ in the visible−NIR region are also due to the electronic transitions in the $U^{V}O_2^{+}$ core.

3.4. Interpretation of the Electronic Spectra of U(V) Complexes. To examine the spectral features of the U(V) complexes in the visible−NIR region from the viewpoint of energy, the electronic spectra of $[U^{V}O_2(dbm)_2DMSO]^{-}$, $[U^{V}O_2(saloph)DMSO]^{-}$, and $[U^{V}O_2(CO_3)_3]^{5-}$ were replotted in wavenumbers (cm^{-1}), as shown in parts a−c of Figure 6, respectively. The peak positions of the characteristic absorption bands of these U(V) complexes are listed in Table 1 in cm^{-1} (the corresponding wavelength values are shown in parentheses). Interestingly, the ϵ values of the characteristic absorption bands of $[U^{V}O_2(CO_3)_3]^{5-}$ are in the range from 0.2 to 3.6 $M^{-1}\cdot cm^{-1}$, while those of $[U^{V}O_2(dbm)_2DMSO]^{-}$ and $[U^{V}O_2(saloph)DMSO]^{-}$ are in the range from 10^2 to ca. 10^3 $M^{-1}\cdot cm^{-1}$. The small ϵ values of $[U^{V}O_2(CO_3)_3]^{5-}$ indicate that the characteristic absorption bands of the U(V) complexes in the visible−NIR region are due to the essentially forbidden electronic transitions in the $U^{V}O_2^{+}$ core. As can be seen from Figure 6 and Chart 1, it is likely that the differences in the ϵ values and the spectral shapes of these U(V) complexes depend on the arrangement of the atoms directly bonded to the center uranium.

A bare $U^{V}O_2^{+}$ ion has a linear geometry, i.e., O═U═O ($D_{\infty h}$). Thus, there is an inversion center in the $U^{V}O_2^{+}$ ion. In this case, electronic transitions between energy states with the same parities ($g \leftarrow g$ and $u \leftarrow u$) in the $U^{V}O_2^{+}$ ion are forbidden by the Laporte selection rule. Even for the U(V) complexes with equatorial ligands, such a selection rule holds in a centrosymmetric system. Assuming that a coordination geometry around the center uranium is approximated by the arrangement of the atoms bonded to the center uranium directly, the center uranium in $[U^{V}O_2(CO_3)_3]^{5-}$ can be regarded as being in a pseudocentrosymmetric hexagonal-bipyramidal field (D_{6h}), while those in $[U^{V}O_2(dbm)_2DMSO]^{-}$ and $[U^{V}O_2(saloph)DMSO]^{-}$ are in noncentrosymmetric pentagonal-bipyramidal ones (D_{5h}). Thus, it is predicted that the absorption bands due to the Laporte forbidden electronic

(25) In the resulting spectrum for the D_2O solution containing $[U^{V}O_2(CO_3)_3]^{5-}$ (5.5×10^{-2} M) and Na_2CO_3 (1 M), the spectrum of HDO was also observed. The HDO was given by the contamination of atmospheric H_2O into the D_2O solution during the bulk electrolysis from $[U^{VI}O_2(CO_3)_3]^{4-}$ to $[U^{V}O_2(CO_3)_3]^{5-}$. Therefore, the spectrum of HDO was subtracted from the resulting spectrum. The broken arrows in Figures 5 and 6c indicate the residuals of the absorption due to HDO.

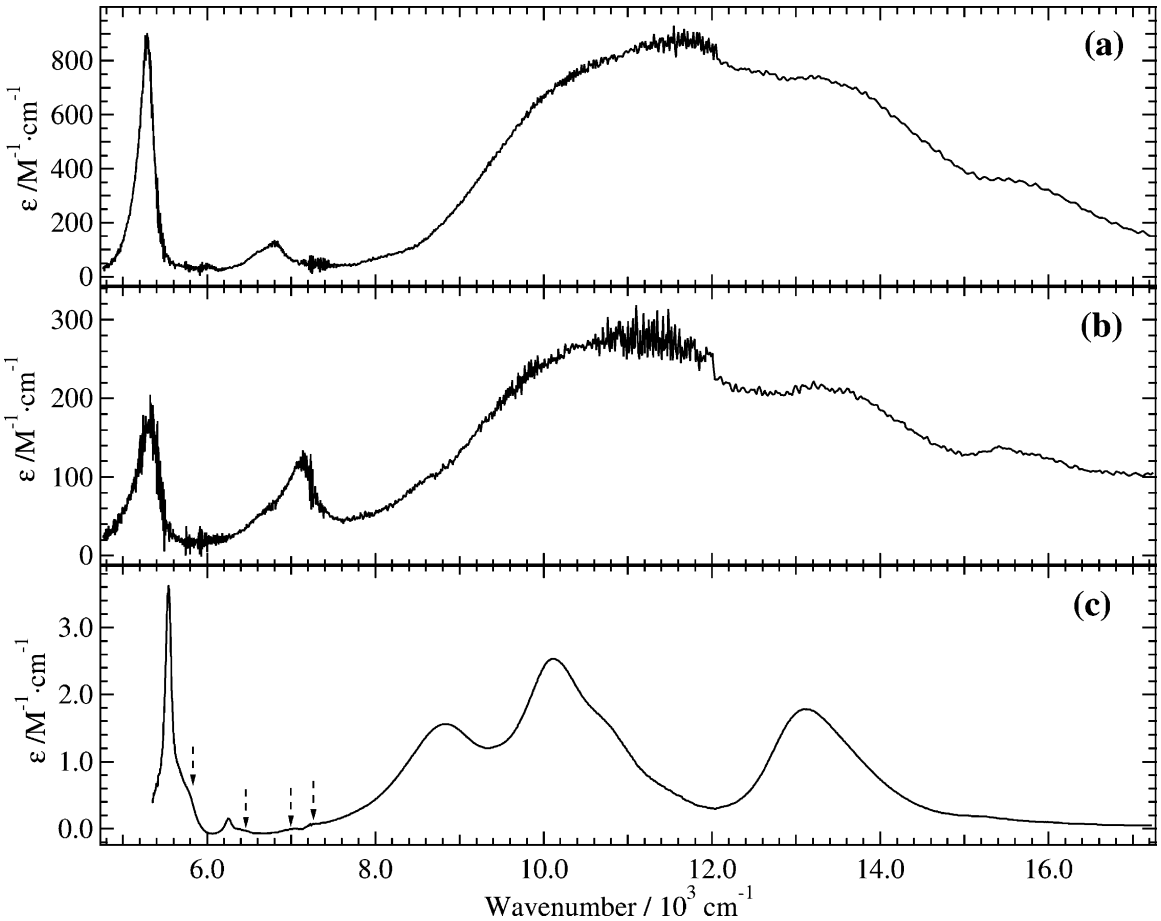

Figure 6. Electronic spectra of U(V) complexes in the visible−NIR region: (a) $[U^VO_2(dbm)_2DMSO]^-$ (4.11×10^{-3} M) in DMSO containing TBAP (0.3 M); (b) $[U^VO_2(saloph)DMSO]^-$ (5.28×10^{-3} M) in DMSO containing TBAP (0.3 M); (c) $[U^VO_2(CO_3)_3]^{5-}$ (5.5×10^{-2} M) in D_2O containing Na_2CO_3 (1 M). Noises in parts a and b are due to detectors (photomultiplier and PbS detector) in the spectrophotometer and/or absorption of DMSO in the OTTLE cell. Broken arrows in part c indicate residuals after subtraction of the spectrum due to HDO from the resulting spectrum.[25] Optical path length: 1.89×10^{-2} cm for parts a and b and 1 cm for part c.

Table 1. Transition Energy Values of f−f Transitions in Actinyl Species with the $5f^1$ Configuration

$U^VO_2^+$ complexes		transition energy/cm^{-1} (nm)					ref
$[U^VO_2(dbm)_2DMSO]^-$		5290 (1890)	6800 (1470)	11600 (860)	13500 (740)	15600 (640)	this work
$[U^VO_2(saloph)DMSO]^-$		5330 (1875)	7140 (1400)	11100 (900)	13300 (750)	15400 (650)	this work
$[U^VO_2(CO_3)_3]^{5-}$		5560 (1800)	6250 (1600)	8770 (1140)	10100 (990)	13200 (760)	this work
$Np^{VI}O_2^{2+}$ species		transition energy/cm^{-1} (term symbol in $D_{\infty h}$)					ref
$[Np^{VI}O_2Cl_4]^{2-}$ ($^2\Delta_{3/2u} + {}^2\Phi_{5/2u}$)[a]	ca. 1000 ($^2\Delta_{3/2u} + {}^2\Phi_{5/2u}$)	6880.4 ($^2\Delta_{5/2u}$)	7990 ($^2\Phi_{7/2u}$)	17241.4 ($^2\Pi_{1/2u}$)	20080.8 ($^2\Pi_{3/2u}$)		38
$[Np^{VI}O_2(NO_3)_3]^-$ ($^2\Phi_{5/2u}$)[a]		6459.0 ($^2\Delta_{5/2u}$)	9420.2 ($^2\Phi_{7/2u}$)	17843.6 ($^2\Pi_{1/2u}$)	20816.3 ($^2\Pi_{3/2u}$)		38
bare $Np^{VI}O_2^{2+}$ ($^2\Phi_{5/2u} + {}^2\Delta_{5/2u}$)[a]	447 ($^2\Delta_{3/2u}$)	5515 ($^2\Delta_{5/2u} + {}^2\Phi_{5/2u}$)	6565 ($^2\Phi_{7/2u}$)	25844 ($^2\Pi_{1/2u}$)	28909 ($^2\Pi_{3/2u}$)		27

[a] Ground state.

transitions in the $U^VO_2^+$ core of $[U^VO_2(dbm)_2DMSO]^-$ and $[U^VO_2(saloph)DMSO]^-$ are observed more strongly than those of $[U^VO_2(CO_3)_3]^{5-}$. This interpretation should explain the differences in the ϵ values in Figure 6. A similar effect of the lack of centrosymmetricity on the intensities of the Laporte forbidden transitions is also confirmed by the theoretical calculations for neptunyl(V) ($Np^VO_2^+$, $5f^2$) complexes with chloride ligands.[26]

For the Laporte forbidden electronic transition scheme in the $U^VO_2^+$ core, there are two candidates; i.e., one is charge transfer from the axial oxygen to the center uranium (LMCT, δ_u, $\phi_u \leftarrow \sigma_u$), and another is a f−f transition ($u \leftarrow u$) in the $5f^1$ electronic configuration. Normally, the U(VI) species show the LMCT absorption bands at around 22 000 cm^{-1} (e.g., the dotted line in Figure 5). Previously, we reported the disappearance of such LMCT bands of $[U^{VI}O_2(CO_3)_3]^{4-}$ with the reduction to $[U^VO_2(CO_3)_3]^{5-}$.[15] In the present study, such a phenomenon was confirmed again, as shown in Figure S1 of the Supporting Information. Because of the lower positive charge on U^{5+} than U^{6+}, it is expected that the LMCT transition in the $U^VO_2^+$ core requires a higher energy

(26) Matsika, S.; Pitzer, R. M. *J. Phys. Chem. A* **2000**, *104*, 11983.

than that in $U^{VI}O_2^{2+}$ (ca. 22 000 cm^{-1}); i.e., a blue shift of the LMCT bands should be observed with the reduction from U(VI) to U(V). Unfortunately, the LMCT bands of $[U^{V}O_2(CO_3)_3]^{5-}$ could not be detected. However, such a blue shift with the reduction from U(VI) to U(V) has been observed in the CsCl−NaCl melt by Khokhryakov (U(VI): 25 000, 31 250, and 33 300 cm^{-1} → U(V): 27 770, 31 764, and 33 300 cm^{-1}).[12] Moreover, according to the quantum chemical calculations for analogous actinyl(V/VI) couples, $Np^{V}O_2^{+}$/$Np^{VI}O_2^{2+}$, by Matsika and Pitzer,[27] the LMCT bands in $Np^{V}O_2^{+}$ appear at a much higher energy region (the lowest transition: 23 079 cm^{-1}) than those in $Np^{VI}O_2^{2+}$ (the lowest one: 12 622 cm^{-1}). Consequently, the characteristic absorption bands of $[U^{V}O_2(dbm)_2DMSO]^{-}$, $[U^{V}O_2(saloph)DMSO]^{-}$, and $[U^{V}O_2(CO_3)_3]^{5-}$ in the visible−NIR region can be assigned to the f−f transitions in the $U^{V}O_2^{+}$ core.

The electronic spectra in Figure 6 might be classified into two regions by the widths of the absorption bands. *Region I*: two narrower absorption peaks in the lower energy side (4800−7600 cm^{-1}). *Region II*: the others with the larger widths (7600−17200 cm^{-1}). According to previous papers,[28−32] it is well-understood for bare actinyl ions that the 5fσ_u and 5fπ_u orbitals are involved in the An═O bonds and hence have antibonding character. On the other hand, the 5fδ_u and 5fϕ_u orbitals in the bare actinyl ion are nonbonding orbitals, which can interact with equatorial ligands. Thus, the typical energy order of the 5f orbitals in the actinyl ions is 5f$\sigma_u \gg$ 5f$\pi_u >$ 5f$\phi_u \approx$ 5fδ_u. Such a relationship should be kept even in the actinyl complexes with ligands in the equatorial plane. Considering the less participation of the 5fδ_u and 5fϕ_u orbitals in the U═O bonding, the narrower absorption peaks in region I are understandable as the electronic transitions from the 5f(δ_u or ϕ_u) orbital[33] to other 5fδ_u and/or 5fϕ_u ones. For region II, the absorption bands might be attributed to the transitions to the 5fπ_u and/or 5fσ_u orbitals because the larger participation of these 5f orbitals in the axial bonding should cause broadening of the spectra. However, it is generally accepted that the 5fσ_u orbital in the actinyl species is lying at a much higher energy level than other 5f orbitals. Thus, the present assignment for the absorption band at the highest energy is a tentative conclusion.

Because Np(VI) species are isoelectronic with U(V) ones ($5f^1$), it is interesting to compare the electronic spectra of the U(V) complexes observed in this study with those of the Np(VI) species. Actually, the Np(VI) species in perchloric[29,34−36] and nitric[37] acid aqueous solutions have their absorption bands at around 6760 and 8330 cm^{-1}. The well-established work for the polarized absorption spectra of the Np(VI) complexes was reported by Denning et al.[38] According to them, $[Np^{VI}O_2Cl_4]^{2-}$ and $[Np^{VI}O_2(NO_3)_3]^{-}$ complexes also have the absorption bands due to the f−f transitions in the visible−NIR region. Furthermore, such experimental data have been compared with the recent quantum chemical calculations for $Np^{VI}O_2^{2+}$ (bare ion) by Matsika and Pitzer.[27] To compare the electronic spectra of the U(V) complexes with those of the Np(VI) species, the energy values of the f−f transitions in the Np(VI) species[27,38] are also collected in Table 1. In this comparison, the absorption band of each U(V) complex in the range of 5290−5560 cm^{-1} should correspond to the second excited state in the f−f transitions. For the Np(VI) species, the first excited state in the f−f transitions is at ca. 1000 cm^{-1}.[27,38] However, such absorption peaks of $[U^{V}O_2(dbm)_2DMSO]^{-}$ and $[U^{V}O_2(saloph)DMSO]^{-}$ have not been observed in the IR spectra of these U(V) complexes.[20,21] The transition energy values of the U(V) complexes in region I are very similar to those of the Np(VI) species. Considering that the participation of the 5fδ_u and 5fϕ_u orbitals in the Np═O bonding is also small, this similarity of the energy values supports our assignment that the absorption peaks of the U(V) complexes in region I are due to the electronic transitions to the 5fδ_u and/or 5fϕ_u orbitals. On the other hand, the transition energy values of the U(V) complexes in region II are much lower than those of the Np(VI) species. Such differences indicate that the antibonding character of the 5fπ_u orbitals in the U(V) complexes is weaker than that in the Np(VI) species. Although the electronic transition to the 5fσ_u orbital in the Np(VI) species has not been observed experimentally, Denning et al. estimated it at 45 000−120 000 cm^{-1} ($^2\Sigma_{1/2u}$), which are not comparable with the absorption bands at around 15 600 cm^{-1} ($U^{V}O_2(dbm)_2DMSO]^{-}$), 15 400 cm^{-1} ($[U^{V}O_2(saloph)DMSO]^{-}$), and 13 200 cm^{-1} ($[U^{V}O_2(CO_3)_3]^{5-}$). Further information should be required for the complete explanation of the characteristic absorption bands of the U(V) complexes in the visible−NIR region. However, it can be concluded that the absorption bands in this region are common features of the actinyl species with the $5f^1$ configuration.

4. Conclusion

In the present study, we have observed the electronic spectra of three types of pure U(V) complexes: $[U^{V}O_2(dbm)_2DMSO]^{-}$, $[U^{V}O_2(saloph)DMSO]^{-}$, and $[U^{V}O_2(CO_3)_3]^{5-}$. As a result, it was clarified that these U(V) complexes have characteristic absorption bands in the visible−NIR region. $[U^{V}O_2(dbm)_2DMSO]^{-}$: 5290, 6800, 11 600, 13 500, and 15 600 cm^{-1} (ϵ = 150−900 $M^{-1}\cdot cm^{-1}$). $[U^{V}O_2(saloph)$-

(27) Matsika, S.; Pitzer, R. M. *J. Phys. Chem. A* **2000**, *104*, 4064.
(28) McGlynn, S. P.; Smith, J. K. *J. Mol. Spectrosc.* **1961**, *6*, 164.
(29) McGlynn, S. P.; Smith, J. K. *J. Mol. Spectrosc.* **1961**, *6*, 188.
(30) Denning, R. G.; Norris, J. O. W.; Short, I. G.; Snellgrove, T. R.; Woodwark, D. R. *Lanthanide and Actinide Chemistry and Spectroscopy*; ACS Symposium Series 131; American Chemical Society: Washington, DC, 1980; pp 313−330.
(31) Hay, P. J.; Martin, R. L.; Schreckenbach, G. *J. Phys. Chem. A* **2000**, *104*, 6259.
(32) Matsika, S.; Zhang, Z.; Brozell, S. R.; Blaudeau, J. O.; Wang, Q.; Pitzer, R. M. *J. Phys. Chem. A* **2001**, *105*, 3825.
(33) It can be expected that the δ_u orbital is positioned lower in energy than ϕ_u because the former (for δ, λ = 2) has the lower angular momentum than the latter (for ϕ, λ = 3). However, their positions may invert for a ligand field and/or a spin−orbit coupling.[27,28,32,38] The electronic configuration at the ground state of each U(V) complex ($5f\delta_u^1$, $^2\Delta_u$; $5f\phi_u^1$, $^2\Phi_u$) was not determined from the present data.
(34) Waggener, W. C. *J. Phys. Chem.* **1958**, *62*, 382.
(35) Eisenstein, J. C.; Pryce, M. H. L. *J. Res. Natl. Bur. Stand.* **1965**, *69A*, 217.
(36) Hagan, P. G.; Cleveland, J. M. *J. Inorg. Nucl. Chem.* **1966**, *28*, 2905.
(37) Friedman, H. A.; Toth, L. M. *J. Inorg. Nucl. Chem.* **1980**, *42*, 1347.
(38) Denning, R. G.; Norris, J. O. W.; Brown, D. *Mol. Phys.* **1982**, *46*, 287.

DMSO]$^{-}$: 5330, 7140, 11 100, 13 300, and 15 400 cm^{-1} (ϵ = 100−300 M^{-1}·cm^{-1}). [$U^{V}O_2(CO_3)_3$]$^{5-}$: 5560, 6250, 8770, 10 100, and 13 200 cm^{-1} (ϵ = 0.2−3.6 M^{-1}·cm^{-1}). From their similarities in the electronic spectra and their differences in the ϵ values, we proposed that the absorption bands of the U(V) complexes are due to the f−f transitions in the $U^{V}O_2^{+}$ core. It should be noted that such an elucidation for the spectroscopic properties of the U(V) complexes has been established by the preparation of the pure U(V) complexes, the observation of their electronic spectra, and the determination of the exact values of the molar absorptivities. These data are the first experimental evidences on the electronic spectral properties of the pure U(V) complexes and will be useful for the deeper understanding of the spectroscopic properties of the actinyl species.

Supporting Information Available: Results of the UV−visible spectroelectrochemical measurements for [$U^{V}O_2(CO_3)_3$]$^{5-}$/[$U^{VI}O_2(CO_3)_3$]$^{4-}$ to evaluate the $E^{\circ\prime}$ value under the present experimental condition.[23] This material is available free of charge via the Internet at http://pubs.acs.org.

IC0503838